CHEMISTRY
A EUROPEAN JOURNAL

DOI: 10.1002/chem.200701867

Mechanistic Insights into the Cobalt-Mediated Radical Polymerization (CMRP) of Vinyl Acetate with Cobalt(III) Adducts as Initiators

Antoine Debuigne,[a] Yohan Champouret,[b] Robert Jérôme,[a] Rinaldo Poli,*[b] and Christophe Detrembleur*[a]

Abstract: Over the past few years, cobalt-mediated radical polymerization (CMRP) has proved efficient in controlling the radical polymerization of very reactive monomers, such as vinyl acetate (VAc). However, the reason for this success and the intimate mechanism remained basically speculative. Herein, two mechanisms are shown to coexist: the reversible termination of the growing poly(vinyl acetate) chains by the $Co(acac)_2$ complex (acac: acetylacetonato), and a degenerative chain-transfer process. The importance of one contribution over the other strongly depends on the polymerization conditions, including complexation of cobalt by ligands, such as water and pyridine. This significant progress in the CMRP mechanism relies on the isolation and characterization of the very first cobalt adducts formed in the polymerization medium and their use as CMRP initiators. The structure proposed for these adducts was supported by DFT calculations. Beyond the control of the VAc polymerization, which is the best ever achieved by CMRP, extension to other monomers and substantial progress in macromolecular engineering are now realistic forecasts.

Keywords: cobalt · density functional calculations · polymerization · radical reactions · vinyl acetate

Introduction

The last few decades have witnessed a huge research effort devoted to techniques able to control the radical polymerization of a variety of monomers.[1] The possible macromolecular engineering of the parent polymers under non-demanding conditions was the basic incentive. Three main techniques of controlled radical polymerization (CRP) have emerged: atom-transfer radical polymerization (ATRP),[2,3] reversible addition–fragmentation chain transfer (RAFT),[4–8] and stable free-radical polymerization (SFRP).[9–12] Other systems must also be mentioned,[13–18] with special emphasis on the so-called "organometallic radical polymerization" (OMRP).[19] In this context, cobalt complexes[20–25] proved highly efficient in mediating the radical polymerization of vinyl monomers, particularly of "nucleophilic" monomers, the radical polymerization of which is not prone to control. For instance, the CRP of vinyl acetate (VAc) was made possible with the assistance of bis(acetylacetonato)cobalt(II), not only in bulk[26] but also in suspension[27] and miniemulsion.[28] This technique, known as cobalt-mediated radical polymerization (CMRP), allows poly(vinyl acetate) (PVAc) and poly(vinyl alcohol) (PVOH, merely upon hydrolysis) to be synthesized with a predetermined molecular weight, and to be constitutive components of block copolymers, which are very difficult to obtain by other techniques.[29–32] Well-defined statistical copolymers[33,34] could also be prepared and fullerene was successfully grafted by PVAc and PVOH.[35]

Until recently, CMRP was explained by a reversible termination mechanism based on the homolytic cleavage of the terminal Co–C bond.[26] However, recent studies proposed that a degenerative chain transfer would operate, at least under certain conditions.[23–25,36] This proposal was supported by the persistent control of the VAc polymerization in the presence of a rather large excess of azo initiator with respect to the cobalt complex, which is typical of a degenerative chain-transfer mechanism.[36] According to the same study,

[a] Dr. A. Debuigne, Prof. R. Jérôme, Dr. C. Detrembleur
Center for Education and Research on Macromolecules
University of Liège
Sart-Tilman, B6a, 4000 Liège (Belgium)
Fax: (+32) 4-366-3497
E-mail: christophe.detrembleur@ulg.ac.be

[b] Dr. Y. Champouret, Prof. R. Poli
Laboratoire de Chimie de Coordination
UPR CNRS 8241 liée par convention à l'Université Paul Sabatier
et à l'Institut National Polytechnique de Toulouse
205 Route de Narbonne, 31077 Toulouse (France)
Fax: (+33) 561-553-003
E-mail: poli@lcc-toulouse.fr

amino derivatives known for coordination to cobalt complexes, such as pyridine, enhanced the reversible termination of the chains.

There is, therefore, a need for an in-depth mechanistic analysis of the CMRP of VAc, which is a prerequisite for further progress in the field. A basic question to be addressed is the structure of the moiety that caps the propagating chains in the dormant state. In this respect, the synthesis of a model compound that is able to initiate the polymerization and to mediate it is of utmost importance. A cobalt adduct would be a reasonable starting point, in a similar manner to alkoxyamines which have proved to be effective initiators and mediators in the SFRP mechanism,[12] although a free-radical initiator and a nitroxide were originally needed to promote this type of controlled polymerization.[9] As the synthesis of cobalt adducts by classical organometallic reactions is a problem, an excess of cobalt(II) acetylacetonate ($Co(acac)_2$) was reacted with radicals generated in the CMRP of VAc. The cobalt species accordingly formed were isolated and characterized with the purpose of collecting a single cobalt adduct. In addition to this synthetic effort, the structure and energy of single model compounds were also investigated by computational tools (DFT studies). Both the experimental observations and the DFT calculations could be unified by quite a consistent mechanism that properly accounts for the effect of the Co ligation on the level of control and kinetics of the VAc polymerization.

Results and Discussion

Synthesis and recovery of cobalt(III) adducts: As previously reported, radical polymerization of VAc falls under control when mediated by $Co(acac)_2$. The ability of this cobalt complex to react with VAc-type radicals and to deactivate them temporarily is the basis of the so-called CMRP. Although the polymerization of VAc initiated by 2,2′-azobis(4-methoxy-2,4-dimethylvaleronitrile) (V-70) at 30 °C is controlled in the presence of $Co(acac)_2$, an induction period of several hours is observed and assumed to be the time needed to generate radicals and convert most of the Co^{II} complex into alkyl cobalt(III) derivatives as result of the trapping of the growing PVAc oligomers.[26,37]

Consistently, the induction period should be suppressed by initiating the CMRP of VAc by a model alkyl cobalt(III) complex. However, alkyl adducts of $Co(acac)_2$ have not been reported in the scientific literature. Nevertheless, a few alkyl cobalt(III) species, mostly model compounds of vitamin B12,[38,39] are well known and have been extensively studied.[40–43] These systems typically feature a planar tetradentate ligand, such as a porphyrin or a Schiff base, which mimics the natural enzyme, an axial alkyl ligand, and an additional axial base *trans* to the alkyl group which completes the octahedral coordination of Co^{III}. Although a limited number of five-coordinate [$CoR(L_4)$] complexes exists,[44] pentacoordination is not a typical occurrence in Co^{III} coordination chemistry, because of the strong ligand field stabilization energy provided by the octahedral coordination for a low-spin d^6 system.[45] It is clear that the synthesis of an alkyl cobalt(III) complex supported by hard-donor ligands, such as acac, is expected to be a difficult task as a result of the sensitivity of the cobalt species to oxygen and temperature (the Co–C bond is quite labile, as assessed by the ability to carry out the polymerization close to room temperature).

Different synthetic strategies were envisioned for the preparation of a model [$Co(acac)_2${-$CH(CH_3)(OCOCH_3)$}] compound, including one-electron oxidative addition of $CH_3CH(OOCCH_3)Br$ to $Co(acac)_2$, generation of $CH_3COOCH(CH_3)^{\bullet}$ radicals from $CH_3CH(OOCCH_3)Br$ and Sn_2Bu_6 or Cu^{I} complexes in the presence of $Co(acac)_2$, and addition of $CH_3CH(OOCCH_3)Br$ to a reduced form of $Co(acac)_2$, but none of these strategies met with success. We therefore turned to the same method used to initiate the polymerization, namely radical generation from V-70, followed by addition of these radicals to the VAc monomer and subsequent trapping with $Co(acac)_2$. The reaction was carried out with an excess of $Co(acac)_2$ with respect to V-70, in order to collect low-molecular-weight cobalt adducts (Scheme 1). Actually, the reaction was stopped before the end of the induction period.

After several hours of reaction at 30 °C, no significant increase in viscosity was observed and the monomer conversion, measured gravimetrically, was close to zero, in agreement with a low polymer content, if any. V-70 residues were eliminated by elution of the crude reaction mixture through silica under an inert atmosphere. Moreover, two fractions were collected with appropriate eluants (see the Experimental Section) and identified as cobalt derivatives by inductively coupled plasma (ICP) mass spectrometry: a minor green compound **1** and a more abundant pink derivative **2**. Formation of two different cobalt species during the induction period was unexpected. Their nature, handling, and ability to initiate and control the polymerization of VAc were systematically investigated.

For reasons that will become apparent after examining the probable structure of product **1**, the above reaction was repeated in the absence of monomer. This procedure led to a final mixture that was worked up in the same way as the mixture leading to the product fractions **1** and **2** above

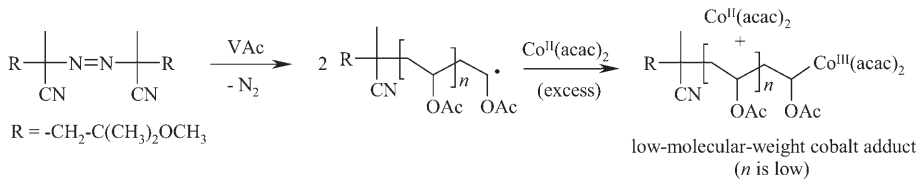

Scheme 1. General strategy for the formation of low-molecular-weight cobalt adducts by CMRP (reaction time < induction period).

(chromatography on a silica column with CH_2Cl_2/EtOAc). A green fraction, the color and elution properties of which are analogous to those of product **1**, was collected, whereas no pink fraction similar to product **2** was obtained in this case.

Characterization of the cobalt(III) adducts

IR characterization: Besides the difference in color and solubility properties (elution through silica), compounds **1** and **2** also differ in their IR properties, as shown in Figure 1. Most notable is the presence of a strong and sharp band centered at 2017 cm^{-1} in the spectrum of product **1**, whereas this band is nearly absent in the spectrum of product **2**. Conversely, **2** shows a strong band centered at 1738 cm^{-1}, whereas this band is very small in the spectrum of **1**. The latter absorption is clearly attributable to an ester function of VAc monomer units, suggesting that product **2** might be the expected Co^{III}-capped PVAc oligomer (Scheme 1). On the other hand, product **1** does not seem to contain monomer units (the small residual band at 1738 cm^{-1} in this product could result from the partial migration of **2** under the elution conditions of **1**). It is for this reason that the reaction between $Co(acac)_2$ and V-70 was repeated in the absence of monomer, leading also to the isolation of compound **1**, as supported by IR spectroscopy (Figure 1). Note that a carbonyl absorption band at 1738 cm^{-1} is completely absent in this case. Thus, product **1** appears to be a byproduct of the CMRP initiating system: V-70 produces primary radicals (R_0) and these are either intercepted by monomer molecules and then terminated by $Co(acac)_2$, leading to the pink [$Co(acac)_2${$(VOAc)_nR_0$}] oligomers **2**, or directly react with $Co(acac)_2$, leading to the green product **1**.

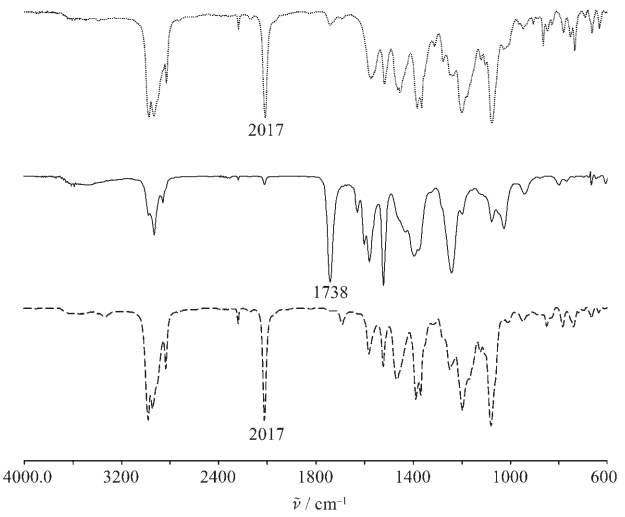

Figure 1. IR spectra of green cobalt adduct **1** (·····) and pink cobalt adduct **2** (——) collected when the reaction between V-70 and $Co(acac)_2$ was carried out in the presence of VAc. IR spectrum of adduct **1** formed by reaction of V-70 and $Co(acac)_2$ without VAc (-----). The cobalt adducts were dissolved in CH_2Cl_2 and solvent-cast on a NaCl disk before IR spectroscopic analysis.

It is reasonable to ask now what the probable structure is for this green material **1**. The absorption at 2017 cm^{-1} is significantly red-shifted from that of a terminal nitrile group (typically in the range 2260–2240 cm^{-1} and is only slightly red-shifted when conjugated with other organic π systems, for example, 2240–2215 cm^{-1} for C=C−C=N and Ar−C=N compounds).[46] The hypothesis of an addition of the primary radical to $Co(acac)_2$ via the carbon atom does not appear reasonable, because on the one hand the CN vibration would not be significantly shifted from that of typical nitrile compounds, and on the other hand, the C−Co bond is not expected to be sufficiently strong (see DFT calculations below). An alternative hypothesis is the addition of the primary radical to $Co(acac)_2$ through the N atom, given that conjugation brings a significant spin density on the N atom, to form a ketiminato ligand (see Scheme 2). A very limited

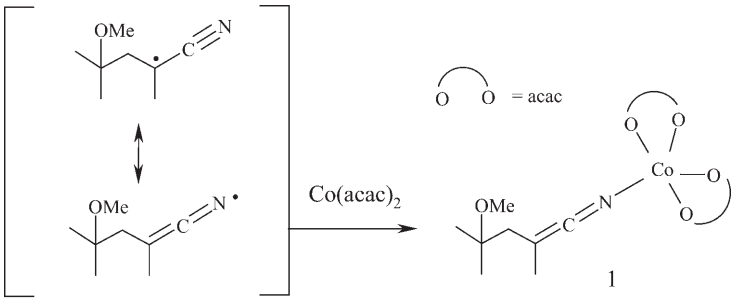

Scheme 2. Hypothesis for the generation and nature of the green product **1**.

number of ketiminato complexes has been previously described, and these exhibit significantly red-shifted C–N stretching vibrations relative to free nitrile functionalities, for example, [IrCp*(N=C=CPh_2)(Ph)(PMe_3)] (ν_{CN} = 2098 cm^{-1}; Cp: cyclopentadienyl)[47] and [$Ru(dmpe)_2$(H)(N=C=CHAr) (Ar = Ph, ν_{CN} = 2120 cm^{-1}; Ar = *p*-$C_6H_4CF_3$, ν_{CN} = 2134 cm^{-1}; dmpe: 1,2-bis(dimethylphosphino)ethane).[48,49]

Independent efforts at crystallizing this product in the form of single crystals suitable for an X-ray diffraction study did not meet with success. The compound appears rather unstable, as it is a thermal source of radicals (see below). During numerous attempts to grow single crystals, mixtures of microcrystalline powder and green crystals were systematically obtained. One of the green crystals, of sufficient quality for an X-ray investigation, turned out to correspond to compound $Co(acac)_3$.[50] The white powder exhibited the typical C–N vibration of terminal nitriles (ν_{CN} = 2240 cm^{-1}). Further information on this decomposition process was obtained by NMR spectroscopy (see below).

DFT investigation of the green ketiminato byproduct: As we were not able to isolate and fully characterize the ketiminato species shown in Scheme 2, that is, the likely candidate for the main product obtained from V-70 and $Co(acac)_2$ as well as the minor product when the same reaction is carried

out in the presence of VAc (product **1**), we decided to explore its structure and energy by computational tools. The calculations were carried out by using the simpler $(CH_3)CH(CN)$ radical in the interests of computational speed.

Qualitatively, one could argue that after formation of the Co–N σ bond, leading to a formally 16-electron $[Co(acac)_2\{N{=}C{=}C(CH_3)_2\}]$ complex, the residual lone pair available on the N atom could interact with an empty Co d orbital and yield a stable five-coordinate complex. This would be an example of the so-called π-stabilized unsaturation.[51] Under the above assumption, the optimization was started from the most reasonable geometry, namely a trigonal bipyramid with the π-donor ligand in the equatorial plane and oriented in such a way as to form the π bond with the (xy, x^2-y^2) set.[52] However, to our surprise, the geometry dramatically rearranged and eventually optimized to a square pyramid with the ketiminato ligand located in one of the equatorial positions (Figure 2). Moreover, this structure is

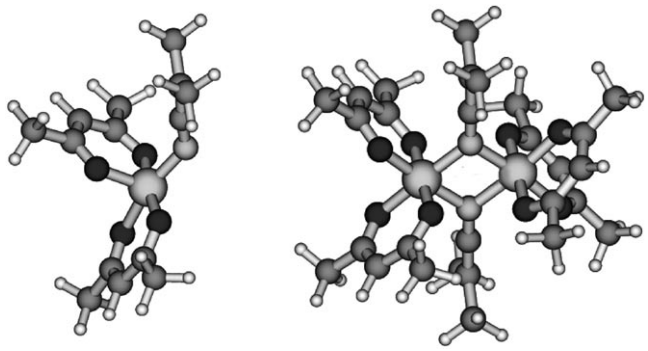

Figure 2. DFT-optimized geometries of mononuclear (left) and dinuclear (right) $[Co(acac)_2\{N{=}C{=}C(CH_3)_2\}]$.

endothermic by 20.0 kcal mol^{-1} relative to the separated $Co(acac)_2$ and $C(CH_3)_2CN$ species, but the calculated C=N frequency would seem in rather good agreement with the experimental value shown in Figure 1. Indeed, the calculation yields 2101 cm^{-1}, versus 2305 cm^{-1} for the C-bonded isomer and 2363 cm^{-1} for the $(CH_3)_2(CN)C{-}N{=}N{-}C(CN)(CH_3)_2$ model of V-70. Against expectations, the optimized Co-N-C angle is very much smaller than 180° (133.4°), clearly indicating that no Co–N π interaction is established. Rather, it appears that the N lone pair is still fully localized on the N atoms and ready to establish a σ bond with a second metal atom.

The above result suggested to us that this mononuclear structure would probably gain in stability by forming a Lewis acid–base dimer. In other words, the N atom of this molecule could donate its lone pair to the Co atom of a second identical molecule, the N atom of which would donate its own lone pair to the Co atom of the first molecule. Indeed, this dinuclear model smoothly optimized to the geometry shown in Figure 2. The system is now exothermic by 9.4 kcal mol^{-1} relative to two $Co(acac)_2$ units and two radicals. Furthermore, the calculated C=N frequencies (2117.5 and 2117.8 cm^{-1}) are once again in line with the experimental value.

NMR characterization: Confirming the conclusions drawn in the IR section, the NMR spectrum of product **1** exhibits far too many resonances, thus indicating that this product is a complex mixture of different compounds. After the first chromatographic separation, the NMR spectrum ($CDCl_3$) exhibits resonances at the expected chemical shift for the acac ligand (singlets at $\delta = 5.52$ and 2.17 ppm) and for the organic groups of R_0 (signals at $\delta = 3.18$ (s), 2.59 (d), 2.19 (d), 1.70 (s), 1.27 (s), and 1.21 (s) ppm), but the spectrum changed and simplified after successive chromatographic purifications. The green fraction contains fewer of the resonances of the organic R_0 fragment and only shows the acac ligand resonances, consistent with the quantitative formation of a diamagnetic Co^{III} species. The white powder mentioned in the IR section was consistent with the simple product of primary radical coupling, R_0–R_0. These results suggest that the ketiminato species suffers from a variety of complex decomposition processes. The detailed mechanism of its decomposition was not further investigated.

The pink cobalt adduct **2** was analyzed by NMR spectroscopy before and after substitution of the $Co(acac)_2$ chain-end by tetramethylpiperdinyloxy free radical (TEMPO; product **2′**). TEMPO is indeed a very efficient scavenger of the PVAc radicals generated by cleavage of the PVAc–Co bond.[53] In this study, adduct **2**, assumed to be a very low-molecular-weight PVAc derivative, was reacted with TEMPO. Comparison of the ^{1}H NMR spectra of **2** and **2′** (Figure 3) confirms the success of the cobalt–TEMPO exchange. The common signals of the two compounds are those of the α end group (V-70 fragment; signals e and f between $\delta = 1.0$ and 1.5 ppm, and signal d characteristic of -OCH_3 at $\delta = 3.16$ ppm) and of the VAc units, the penultimate unit excluded (signal a corresponding to C*H*OAc between $\delta = 4.8$ and 5.2 ppm, and signal b corresponding to CH_2, mixed with other signals between $\delta = 2.0$ and 1.7 ppm). The signals of the PVAc final unit and those of the chain end attached to such a unit differ as expected. For the sake of clarity, those of compound **2′** are described first. The protons corresponding to TEMPO can be observed between $\delta = 1.0$ and 1.5 ppm (signals i and j in Figure 3b). Moreover, signal h, corresponding to the C*H*OAc proton in the final VAc unit, linked to the TEMPO, is shifted downfield to $\delta =$ 6.2 ppm. The latter signal, on the other hand, is absent in the spectrum of **2** and is replaced by a resonance at $\delta =$ 2.5 ppm. This spectacular upfield shift is related to the replacement of the electronegative O atom with the electropositive Co atom. The rather large width of resonance h in both spectra is due to the expected presence of several contributing species. Firstly, the dyad made up of the two last monomer units may be of r or m type. The r dyad has a CH_2 group with equivalent H atoms, giving rise to a triplet, while the CH_2 group of the m dyad has diastereotopic H atoms, giving rise to a doublet of doublets. Radical polymerization

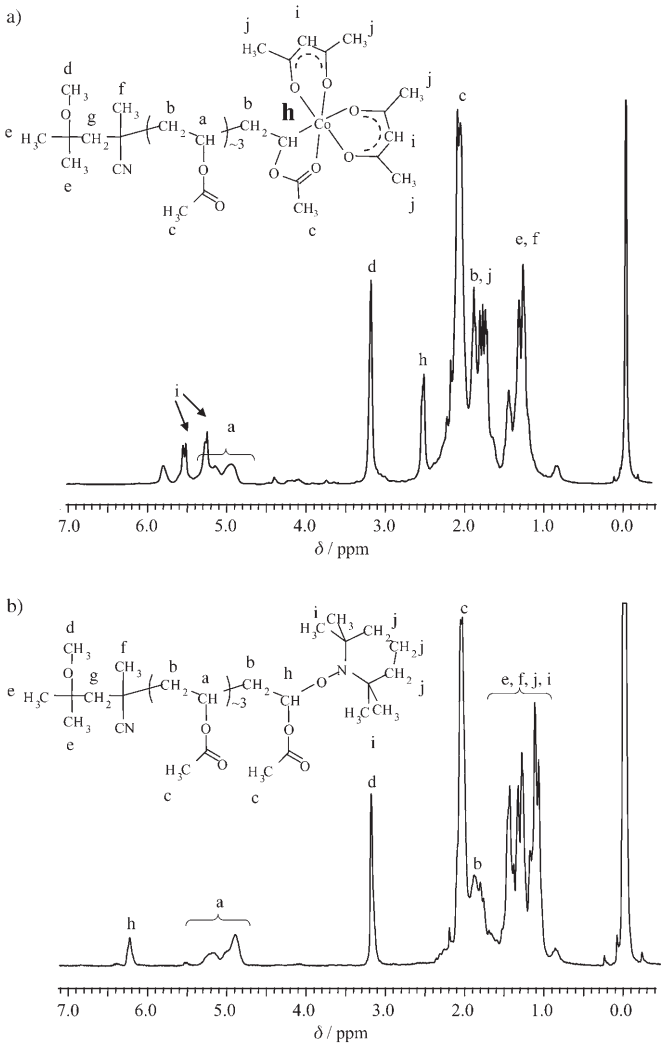

Figure 3. ^{1}H NMR spectrum for the low-molecular-weight cobalt adduct **2**: a) untreated; b) after treatment with TEMPO (**2′**). Solvent: $CDCl_3$.

is nonstereospecific and the two dyads are expected in an approximately 1:1 ratio. Secondly, the number of distinct species is further doubled by an additional diastereomeric relationship resulting from the chirality of the cobalt center (see below).

It is now interesting to observe that the acac ligands of the $Co(acac)_2$ chain-end are not equivalent, with the two main i resonances for the C*H* groups observed at $\delta = 5.5$ and 5.3 ppm. This suggests a *cis* arrangement for the two acac groups in a pseudo-octahedral arrangement, rendering the Co center chiral. The slight splitting observed for the i resonances may be attributed to the presence of two different diastereoisomers, differing from the relative configurations of the Co atom and Co-bonded C atom, as mentioned above. The corresponding CH_3 resonances (j) overlap with other resonances in the $\delta = 2.0$ to 1.4 ppm region. This bonding picture is fully supported by DFT calculations, which are described in a later section. The average number of VAc units in the pink cobalt adduct **2** is close to four, as calculated from the intensity of the proton resonances typical of the VAc units and the chain ends, respectively. In conclusion, compound **2** is a very low-molecular-weight cobalt adduct formed by the rapid trapping of the growing PVAc chains by $Co(acac)_2$, as suggested in Scheme 1.

UV/Vis characterization: The green cobalt adduct **1** and the pink derivative **2** were also discriminated by UV/vis spectroscopy under an inert atmosphere (Figure 4). An absorption maximum was observed at $\lambda = 592$ nm for the minor product **1** and at $\lambda = 516$ nm for compound **2**.

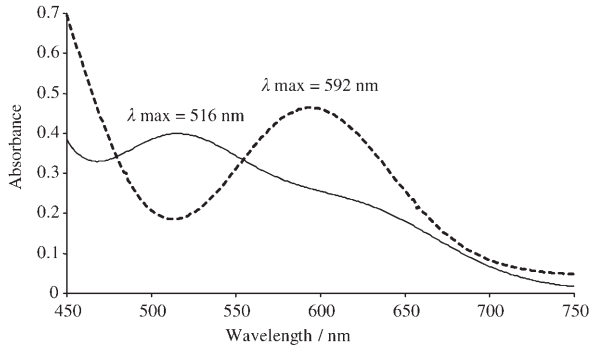

Figure 4. UV/vis spectra for the green compound **1** (-----, $\lambda_{max} = 592$ nm) and pink compound **2** (——, $\lambda_{max} = 516$ and 613 nm) in degassed CH_2Cl_2.

Moreover, the absorption profiles changed when these cobalt complexes were handled under different conditions. For example, the pink compound **2** turned green when not purified under an inert atmosphere, whereas the coloration of compound **1** did not change. The sensitivity of the low-molecular-weight PVAc–$Co^{III}(acac)_2$ compound **2** to oxygen was confirmed by the continuous change of the UV/vis spectrum upon exposure to air (Figure 5), together with a color change from pink to green. After one hour, the UV/vis curve no longer changed, consistent with the complete conversion of the pink compound **2** into a green product **3**. The latter compound is, however, different from the minor green

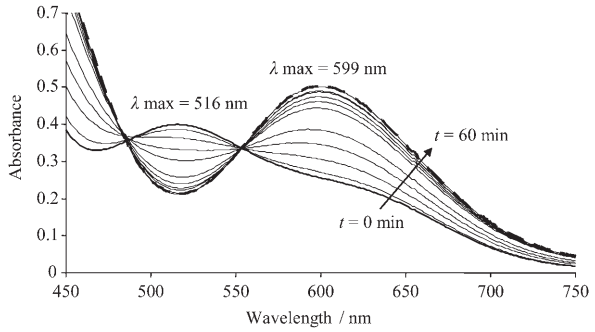

Figure 5. Evolution of the UV/vis spectrum of the pink compound **2** (broad full line, $\lambda_{max} = 516$ nm) in degassed CH_2Cl_2 when exposed to air. Spectra were collected every 5 min for 60 min until the color turned green (compound **3**, broad dashed line, $\lambda_{max} = 599$ nm).

product **1**, the λ_{max} of compound **3** being $\lambda = 599$ nm instead of $\lambda = 592$ nm for compound **1** (Figure 5).

The UV/vis spectrum of compound **2** does not change upon addition of distilled and degassed water as long as the sample is maintained under an inert atmosphere (Figure 6).

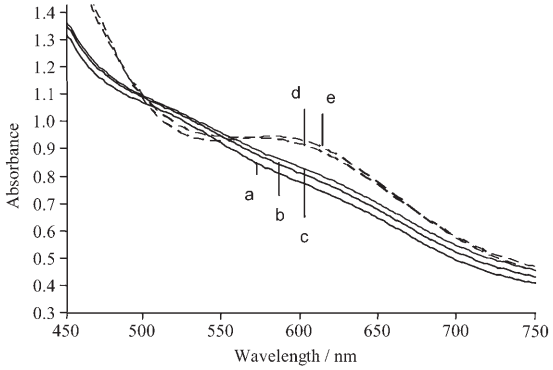

Figure 6. Evolution of the UV/vis spectrum of the pink cobalt adduct **2** in a degassed acetone/water mixture (9.5:0.5; ——), a) $t = 0$, b) $t = 20$, c) $t = 40$ min under an inert atmosphere, before exposure to air for 4 min between each scan (-----) at d) $t = 60$ and e) $t = 100$ min.

In contrast, upon exposure to air, the pink solution **2** turns green, as previously observed. It is thus clear that oxidation is basically responsible for the conversion of the low-molecular-weight cobalt adduct **2** into the green compound **3**, and not coordination of water (air moisture) onto cobalt with formation of a six-coordinate cobalt chain end [$Co(acac)_2$-(H_2O)(PVAc)]. A likely first step of the chemical transformation responsible for the color change is the insertion of a dioxygen molecule into the Co–C bond, to yield an alkylperoxo complex, which then may evolve to other products. A characteristic example of this oxidation process was reported elsewhere, including the X-ray analysis of the alkylperoxo product.[54]

Polymerization of VAc initiated by the cobalt(III) adducts: A key question to address is the ability of the isolated Co adducts **1–3** to initiate the CMRP of VAc and, in the case of success, to control it. This study should allow determination of whether or not the initiation of CMRP takes place according to a degenerative chain-transfer mechanism or by simple cleavage of the cobalt–carbon bond and release of the initiating radical (Scheme 3).

Radical polymerization of VAc was carried out with compounds **1–3** and the data are reported in Table 1. When performed at 30 °C in the presence of the green product **1**, the polymerization of VAc is rather fast (10 % conversion per hour) although uncontrolled (Table 1, entry 1). Indeed, the molar mass is much higher than expected in the case of control, and it does not increase with monomer conversion beyond 20 %. The polydispersity of PVAc was also high (≈ 2). That the initiator efficiency is low is not surprising in the light of the thermal decomposition process revealed by the above-described spectroscopic studies. The complexity of the decomposition reaction, which releases Co^{III} products together with $Co(acac)_2$, also accounts for the poor control of the process. Nevertheless, compound **1** is able to form primary radicals under mild conditions but their actual structures are unknown.

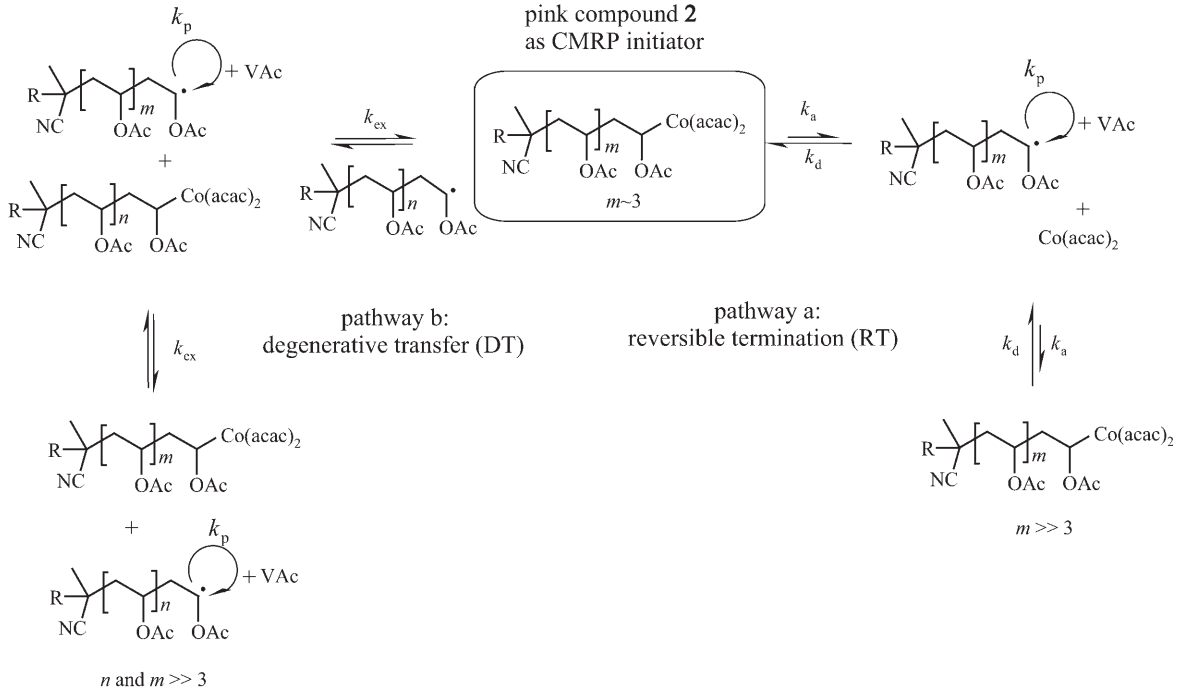

Scheme 3. Possible mechanisms of reversible termination and degenerative chain transfer in the CMRP of VAc initiated by a model cobalt adduct.

Table 1. CMRP of VAc initiated by different cobalt adducts.[a]

Entry	t [h]	Conversion [%]	$M_{n,SEC}$[b] [g mol^{-1}]	$M_{n,th}$[c] [g mol^{-1}]	M_w/M_n[d]
1	1	12.5	32200	3980	2.25
	2	25.6	50400	8600	1.88
	3	33.7	54800	11300	1.84
	4	40.0	55600	13200	1.89
2	1	3.0	907	620	1.20
	2	4.4	1120	902	1.24
	4	7.9	2180	1620	1.07
	6	9.3	2860	1900	1.07
	7	11.3	3400	2320	1.07
3	24	–	–	–	–

[a] Bulk polymerization at 30 °C. 1) Green compound **1** (0.140 mmol)/VAc (54.0 mmol); 2) pink compound **2** (0.227 mmol)/VAc (54.0 mmol); 3) green compound **3** (0.227 mmol; resulting from exposure of **2** to air for 16 h)/VAc (54.0 mmol). [b] The number-average molecular weight determined by size-exclusion chromatography ($M_{n,SEC}$) in THF with a polystyrene (PS) calibration. [c] Theoretical molar mass calculated from the [VAc]/[Co] ratio and conversion. The cobalt concentration was determined by ICP. [d] M_w: weight-average molecular weight.

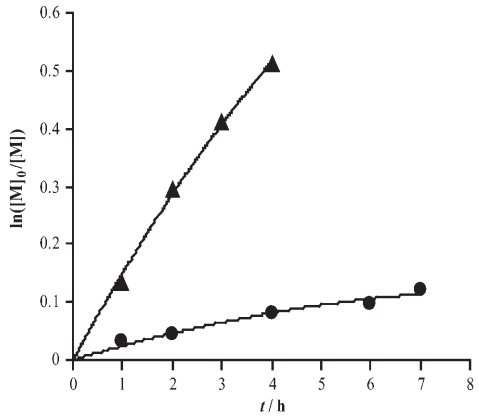

Figure 7. Time dependence of $\ln[M]_0/[M]$ (M: monomer) for VAc polymerization initiated by compound **1** (▲) and compound **2** (●); Table 1, entries 1 and 2, respectively.

Table 2. CMRP of VAc initiated by the pink cobalt adduct **2** in the presence of V-70 at 40 °C.[a]

	t [h]	Conversion [%]	$M_{n,SEC}$[b] [g mol^{-1}]	$M_{n,th}$[c] [g mol^{-1}]	M_w/M_n
1	1	3.7	–	–	–
	2	4.0	7800	10000	1.10
	3	6.6	16600	16600	1.05
	4	8.4	20100	21100	1.07
	5	9.9	23800	24900	1.08
2	1	8	16600	20100	1.11
	2	16	32300	40200	1.14
	3	33	63500	83000	1.25
	4	49	78000	123100	1.31
	5	55	94700	138200	1.43

[a] At 40 °C. Adduct **2**, 0.0185 mmol (determined by ICP). 1) VAc, 54.0 mmol; 2) VAc (54.0 mmol)/V-70 (0.02 mmol); [Co]/[V-70] = 0.925. [b] $M_{n,SEC}$ in THF with a PS calibration. [c] Calculated from the [VAc]/[Co] ratio and conversion. The cobalt concentration was determined by ICP.

In contrast, the polymerization of VAc conducted with the pink cobalt adduct **2** is very slow and controlled (Table 1, entry 2). Indeed, the monomer conversion is only 11 % after 7 h, whereas the molar mass increases regularly with monomer conversion. There is a rather good agreement between the experimental and theoretical molar masses, and the polydispersity is low along the polymerization ($\approx$1.1–1.2). Thus, it appears that the alkyl cobalt complex **2** is a realistic model for the PVAc–Co(acac)$_2$ dormant chains. The initiation of the polymerization and the slow consumption of VAc in the presence of the purified compound **2** are accounted for by the homolytic cleavage of the C–Co bond and the occurrence of a reversible termination process (pathway a, Scheme 3). However, for the time being, it cannot be excluded that a propagating chain, released by the reversible termination mechanism, is involved in a degenerative chain-transfer process.

The kinetics of the polymerizations carried out with the cobalt adducts **1** and **2** are compared in Figure 7, which clearly emphasizes a much higher polymerization rate in the case of complex **1**.

Polymerization of VAc initiated by the pink alkyl cobalt complex 2 in the presence of additives

Addition of V-70: It was recently suggested that bulk CMRP of VAc proceeds by a degenerative chain-transfer mechanism (pathway b, Scheme 3) when conducted in the presence of V-70. To give credit to this proposal, the VAc polymerization was initiated by adduct **2** in the presence of V-70 (Table 2). As expected, the addition of V-70 to the polymerization medium dramatically increases the polymerization rate (entries 1 and 2 in Table 2). $M_{n,SEC}$ increases regularly with the monomer conversion, as expected for a controlled process. Nevertheless, the polydispersity also increases with the progress of polymerization, which indicates that the control is not ideal. All in all, these observations support the notion that a degenerative chain-transfer process contributes to the polymerization in the presence of additional azo initiator.

Addition of pyridine: Another way to speed up CMRP while maintaining the polymerization control consists of adding electron-donating compounds, such as pyridine.[36] Indeed, it was reported that bulk CMRP of VAc initiated by V-70 in the presence of Co(acac)$_2$ was faster and that the induction period disappeared in the presence of pyridine, which is able to coordinate the cobalt complex. It was suggested that this ligand changes the polymerization mechanism from a degenerative chain transfer to a reversible termination process. In this work, a small amount of pyridine was added to adduct **2**. As expected, the polymerization was three times faster when conducted in the presence of a stoichiometric amount of pyridine with respect to the cobalt complex (Table 3 and Figure 8a).

Table 3. CMRP of VAc initiated by the pink cobalt adduct **2** in the presence of pyridine.[a]

t [h]	Conversion [%]	$M_{n,SEC}$[b] [g mol^{-1}]	$M_{n,th}$[c] [g mol^{-1}]	M_w/M_n
1	9	3140	1950	1.06
3	18	5500	3700	1.06
5	25	7100	5100	1.07
7	29	8600	6000	1.07
24	54	15400	11100	1.09
30	61	17000	12300	1.10

[a] Bulk polymerization at 30 °C. Adduct **2** (0.227 mmol)/VAc (54.0 mmol)/pyridine (18 mg, 0.229 mmol). [b] $M_{n,SEC}$ in THF with a PS calibration. [c] Calculated from the [VAc]/[Co] ratio and conversion. The cobalt concentration was determined by ICP.

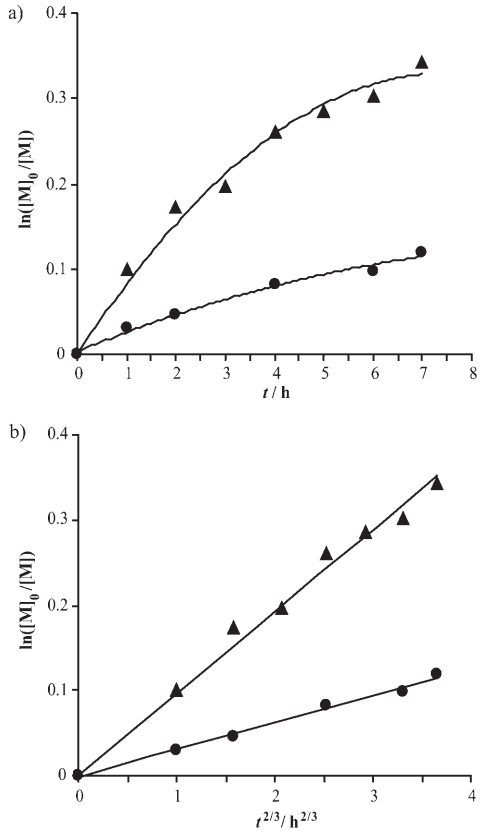

Figure 8. a) First- and b) 2/3-order dependence of ln[M]$_0$/[M] on time for VAc polymerization initiated by compound **2** with (▲) and without (●) pyridine; Table 3 and entry 2 of Table 1, respectively.

The power law in Equation (1) was investigated:

$$\ln[M]_0/[M] = (3k_p/2)(K[P\text{-}X]_0/3k_t)^{1/3}\, t^{2/3} \quad (1)$$

in which k_p and k_t are the rate constants of propagation and termination, respectively, K is the equilibrium constant between the active and the dormant species, and P-X stands for the polymeric dormant species end-capped by the control agent X.

This power law was experimentally observed for polymerizations directly initiated by alkoxyamines, in the absence of conventional radical initiator and free nitroxide.[55–57] In a similar manner to alkoxyamines, adduct **2** releases both the initiating radical and the controlling agent ($Co(acac)_2$). Therefore, it is not surprising to observe a linear 2/3 order dependence of ln[M]$_0$/[M] on time for the polymerization carried out with this compound. This observation is additional evidence that a reversible-termination mechanism operates in the controlled process.

Under these conditions, the polydispersity remains very low (1.10) and the molar mass increases with the monomer conversion. The clear shift of the size-exclusion chromatograms towards shorter elution times when the monomer conversion increases is shown in Figure 9.

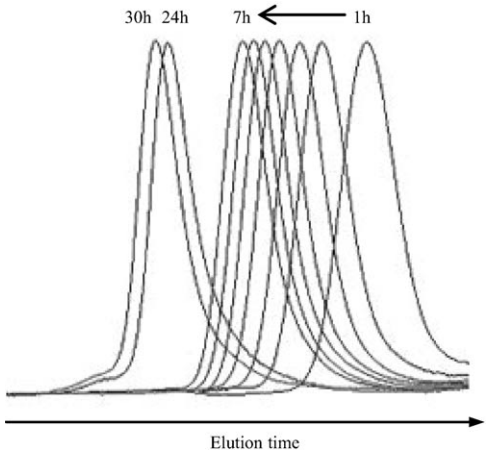

Figure 9. Evolution of size-exclusion chromatograms with time for VAc polymerization initiated at 30 °C by adduct **2** in the presence of a stoichiometric amount of pyridine (Table 3).

Addition of water: Ligation of $Co(acac)_2$ by water molecules was also previously suggested. Therefore, adduct **2** was used in conjunction with water in the CMRP of VAc. The addition of water has a beneficial effect on the polymerization kinetics (compare Table 1, entry 2 and Table 4). Indeed, after 7 h, the monomer conversion increases from 11 to 52 % upon addition of water. Figure 10a is another illustration of this strong kinetic effect.

Table 4. CMRP of VAc initiated by the pink cobalt adduct **2** in the presence of water.[a]

t [h]	Conversion [%]	$M_{n,SEC}$[b] [g mol^{-1}]	$M_{n,th}$[c] [g mol^{-1}]	M_w/M_n
1	19	4900	3900	1.11
2	29	6700	5900	1.10
3	36	7800	7400	1.08
4	41	8900	8300	1.07
5	45	9700	9200	1.07
7	52	11700	10600	1.06
24	97	19300	19800	1.12

[a] Bulk polymerization at 30 °C. Compound **2** (0.227 mmol)/VAc (54.0 mmol)/H_2O (2.22 mmol). [b] $M_{n,SEC}$ in THF with a PS calibration. [c] Calculated from the [VAc]/[Co] ratio and monomer conversion. The cobalt concentration was determined by ICP.

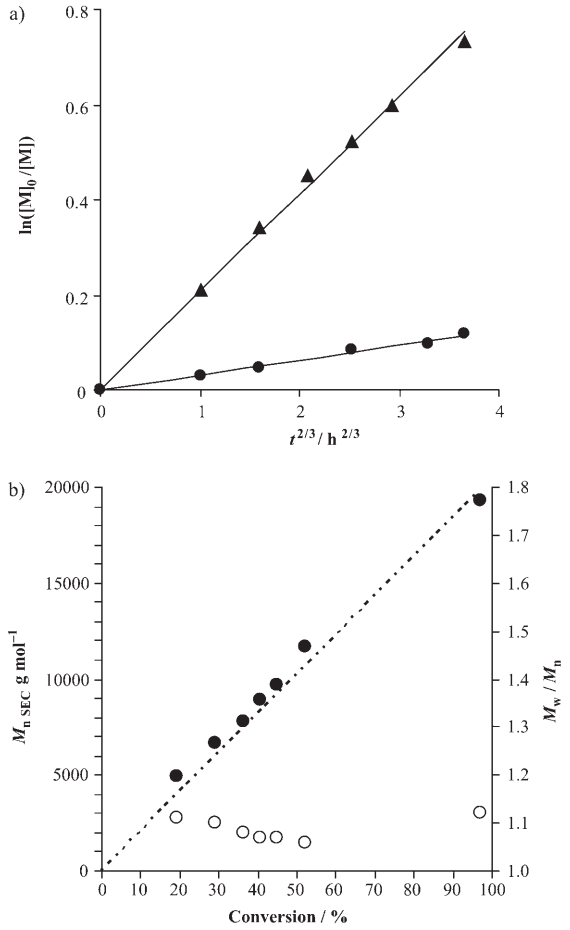

Figure 10. a) 2/3-order time dependence of $\ln[M]_0/[M]$ for VAc polymerization initiated by the adduct **2** with (▲) and without (●) water (Table 4 and entry 2 in Table 1, respectively). b) Dependence of the molar mass (●) and molar mass distribution (○) for VAc polymerization initiated by adduct **2** in the presence of water (Table 4). —— is the theoretical prediction based on the [VAc]/[Co] ratio.

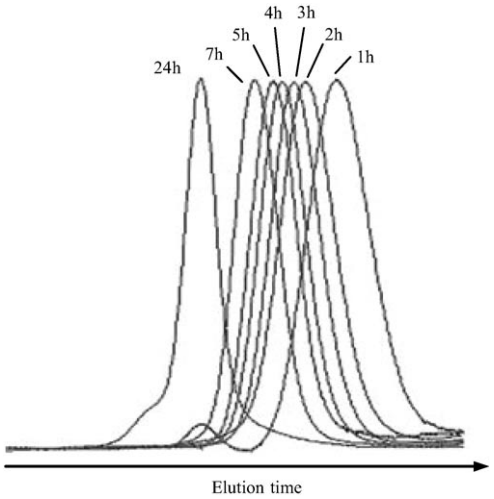

Figure 11. Evolution of the size-exclusion chromatograms of PVAc with the polymerization time. This polymerization was initiated by adduct **2** added with water at 30 °C (Table 4).

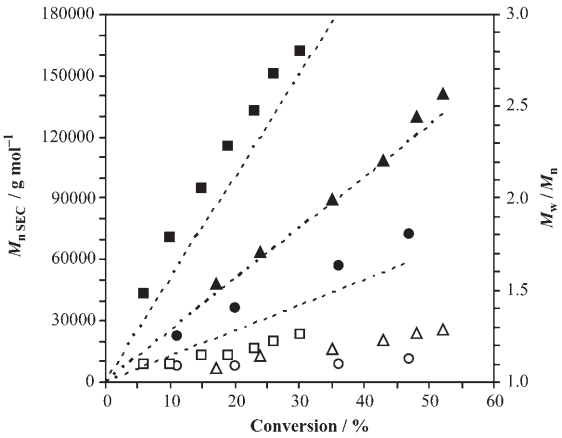

Figure 12. Dependence of the molar mass (filled symbols) and molar mass distribution (empty symbols) on monomer conversion for VAc polymerization initiated by adduct **2** in the presence of water, at different [VAc]/[Co] ratios. —— corresponds to the theoretical molar masses calculated from the [VAc]/[Co] ratios and VAc conversions. Conditions: 40 °C, adduct **2** (0.0185 mmol), H_2O (2.22 mmol), VAc (●: 27.0, ▲: 54.0, ■: 108.0 mmol).

Moreover, the experimental data reported in Table 4 agree with a controlled polymerization as assessed by the linear relationships between M_n and the monomer conversion (Figure 10b) and between $\ln[M]_0/[M]$ and $t^{2/3}$ (Figure 10a). This 2/3-order linear dependence gives credit to a controlled polymerization that proceeds by a reversible termination mechanism in the presence of water.[58–60] Furthermore, the polydispersity is very low ($\approx$1.1) and the molar masses are very close to the theoretical values, even at monomer conversions as high as 97 %. The excellent level of control imparted to the VAc polymerization by water is nicely illustrated by the shift of the size-exclusion chromatograms towards shorter elution times (Figure 11).

At constant $[H_2O]/[\mathbf{2}]$ ratio, the PVAc molar mass is controlled as expected by the [VAc]/[**2**] ratio (see Figure 12). Note that PVAc with a molar mass as high as 160 000 g mol^{-1} and a low polydispersity (1.3) can be prepared in a controlled manner. The level of control is, therefore, higher when conducted with the cobalt model compound **2** than with a combination of $Co(acac)_2$ and V-70.

Impact of water on the course of the CMRP of VAc: The effect of water on the CMRP of VAc discussed above was an incentive to revise the discussion of previously reported experiments of CMRP in suspension[27] and miniemulsion.[28] When carried out by these techniques rather than in bulk, the VAc polymerization was typically much faster while remaining under control. This effect was tentatively explained by the diffusion of the control agent ($Co(acac)_2$) from the monomer droplets to the aqueous phase, which shifted the equilibrium between active and dormant species towards the active ones. Although this compartmentalization effect cannot be precluded, the ability of water to coordinate the cobalt complex must be taken into account. In this respect,

a series of experiments was carried out to discriminate these two effects (Figure 13).

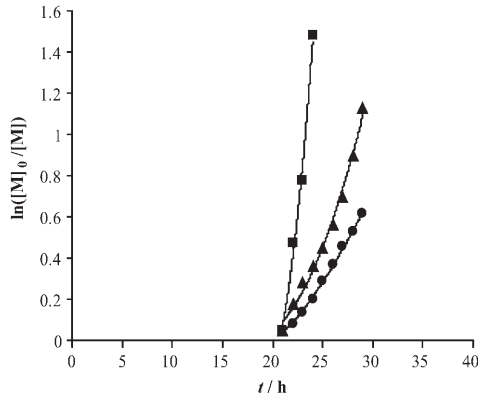

Figure 13. Plot of $\ln([M]_0/[M])$ versus time t for VAc polymerization in the presence of $Co(acac)_2$ at 30 °C. Conditions: 21 h of pre-reaction, [VAc]/[$Co(acac)_2$]/[V-70] = 540:1:3 then (●) no water added, (▲) water-saturated VAc (■), or biphasic system: $V_{VAc}/V_{H_2O} = 4$.

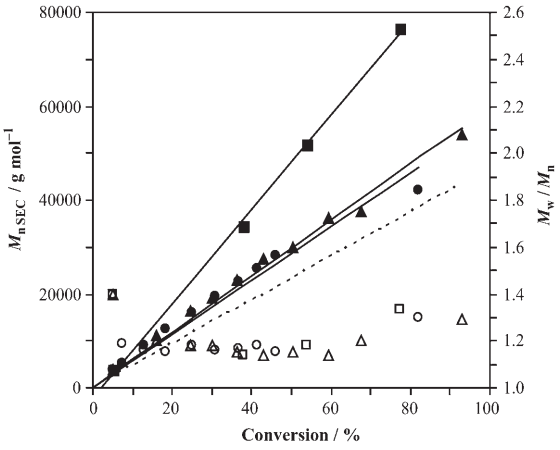

Figure 14. Dependence of the molar mass (filled symbols) and molar mass distribution (empty symbols) on monomer conversion for VAc polymerization in the presence of $Co(acac)_2$ at 30 °C. Conditions: 21 h of pre-reaction, [VAc]/[$Co(acac)_2$]/[V-70] = 540:1:3 then (●/○) no water added (f = 0.82), (▲/△) water-saturated VAc (f = 0.78), or (■/□) two-phase system: $V_{VAc}/V_{H_2O} = 4$ (f = 0.46); $f = M_{n,th}/M_{n,SEC}$.

Right after the induction period, as soon as the bulk CMRP of VAc started, the reaction medium was split into three parts. The first one was merely maintained at 30 °C. The dry VAc of the second portion was evaporated and replaced by VAc saturated with water. A large volume of water ($V_{VAc}/V_{H_2O} = 4$) was added to the third fraction, which phase-separated immediately. The significantly faster polymerization when water-saturated VAc was substituted for dry VAc has to be accounted for by water coordination to the cobalt complex. This kinetic benefit was, however, much smaller than the one observed when the experiment was carried out with a large amount of water, which mimics the suspension/miniemulsion conditions. Only an equilibrium displacement in favor of the active species, triggered by diffusion of $Co(acac)_2$ to the aqueous phase, can explain the amplification of the kinetic effect. In all three cases, the VAc polymerization fits a controlled pattern as assessed by the linear dependence of M_n on the monomer conversion and the rather low polydispersity (1.15–1.3; Figure 14). The much more important discrepancy between theoretical and experimental molar masses observed for the biphasic system is more likely a consequence of the compartmentalization effect, as was observed for CMRP in aqueous dispersed media.

Theoretical investigations into the nature of the organometallic chain end in the dormant species: Our attempts to generate, isolate, and characterize a model compound of the PVAc–$Co(acac)_2$ "unimer" have so far been unsuccessful, as detailed in a previous section. For this reason, we turned to a computational study of the [$Co(acac)_2${-$CH(CH_3)$-($OCOCH_3$)}] unimer model. The question is whether this compound would be sufficiently stable relative to the separated $CH_3CH(OOCCH_3)$ and $Co(acac)_2$ species and whether it adopts a five- or six-coordinate geometry. When the polymerization is carried out in the presence of additional bases (L), such as water or pyridine, and the reaction follows a reversible termination mechanism (see above), one molecule of the base probably adds to the Co center in the dormant species to afford a [$Co(acac)_2$(L)(PVAc)] chain end. However, in the absence of added bases, that is, when the polymerization follows most probably a degenerate transfer mechanism, the structure of the cobalt chain end is less certain. In a recently published study, some of us reported DFT calculations on a model CH_3–$Co(acac)_2$ system.[36] The system was found to be most stable in a square pyramidal geometry with the CH_3 group in the axial position and with a spin singlet configuration, its enthalpy value being −14.55 kcal mol^{-1} relative to the separated CH_3 radical and $Co(acac)_2$ (which adopts a tetrahedral coordination geometry with a spin quartet ground state). That is, the bond dissociation enthalpy BDE(Co–CH_3) = 14.55 kcal mol^{-1}. Furthermore, axial coordination of ligands such as pyridine, NH_3, or H_2O further stabilized the system by an additional 9–13 kcal mol^{-1}.

In the present study, we wish to address the nature of the dormant species $CH_3CH(X)$–$Co(acac)_2$, not only when X = $OOCCH_3$, the model of the PVAc–$Co(acac)_2$ unimer, but also when X = $COOCH_3$ and OCH_3, to model growing poly(methyl acrylate) (PMA) and poly(vinyl methyl ether) (PVME) chains, respectively. The PMA model was selected because it was previously reported that $Co(acac)_2$ is ineffective in controlling the polymerization of methyl acrylate (MA).[26] The other model (PVME) is of interest because previously published DFT calculations showed that its bonds with halides[58] and dithiocarboxylates[59] are nearly as strong as those established by the PVAc model. Finally, we also modeled an R–$Co(acac)_2$ compound with R = C-(CH_3)$_2$CN as a simpler model (in the interests of computational time) of the primary radical generated from V-70, to

assess the possibility that $Co(acac)_2$ could directly trap this radical.

All R–$Co(acac)_2$ systems give similar optimized geometries to that previously reported with R=CH_3 (see Figure 15). The BDE(Co–R) energies are reported in

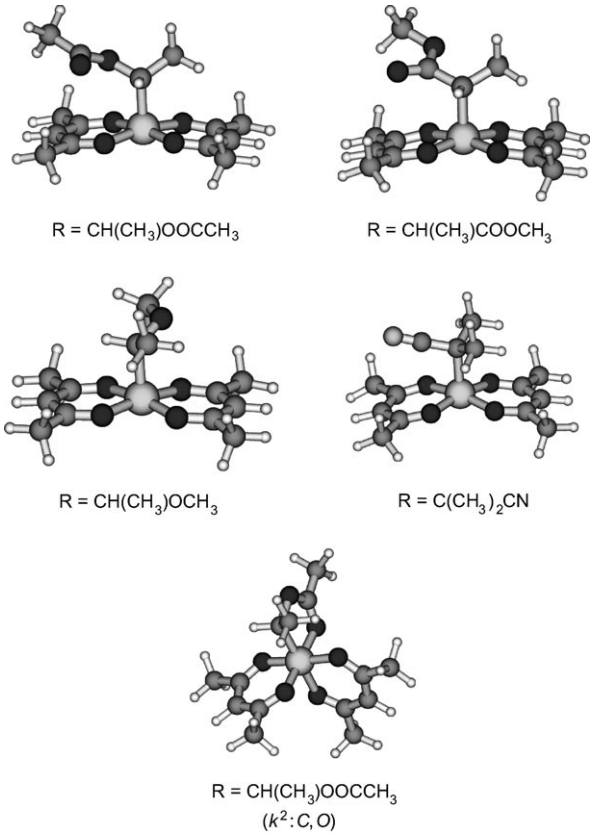

Figure 15. DFT-optimized geometries of the model compounds R–$Co(acac)_2$.

Table 5, together with the Co–C bond lengths. As expected, all systems show weaker Co–C bonds than the previously reported methyl compound. The BDE decreases when X varies in the order OMe > $OOCCH_3$, but all these values are still positive. On the other hand, the PMA unimer model yields a negative value. This result is in good agreement with the experimental observation that the MA polymerization cannot be controlled in the presence of $Co(acac)_2$, that is, this compound is not a good spin trap for the PMA growing radical chain. The model of the V-70 primary radical also gives a negative BDE. This is expected from the highly stabilized nature of the resulting radical (tertiary carbon atom, conjugation with the CN group), and illustrates the principle that the primary radicals are not likely to be trapped by $Co(acac)_2$ with formation of Co–C bonds. Rather, they are trapped by formation of Co–N bonds (see above). Note that cobalt porphyrin complexes are capable of controlling the polymerization of MA,[20] suggesting that the Co–R bonds are stronger in the presence of a porphyrin ancillary ligand. A theoretical investigation of ancillary ligand effects on the Co–R BDE, however, is beyond the scope of the present work. From Table 5, it can be seen that the optimized Co–C bond length does not correlate in a simple way with the Co–C homolytic bond strength. For instance, whereas the bond is expectedly longer for the weaker bond (with $C(CH_3)_2(CN)$) and shorter for the stronger bond (with CH_3), the system with $CH(CH_3)OCH_3$ also shows a rather long bond. Although one may invoke the different contribution of steric, polar, and resonance effects in determining strength on one side and length on the other, the way in which these effects operate is not obvious to deduce from these limited data.

Table 5. Co–R bond dissociation enthalpies and relevant optimized geometrical parameters for the R–$Co(acac)_2$ molecules.

R	Co–R BDE [kcal mol^{-1}]	Co–R distance [Å]
CH_3[a]	14.55	1.921
$CH(CH_3)OCH_3$	8.45	1.987
$CH(CH_3)OOCCH_3$	5.73	1.957
$CH(CH_3)OOCCH_3$ (κ^2:C,O)	11.92	1.997
$CH(CH_3)COOCH_3$	−1.50	1.983
$C(CH_3)_2CN$	−5.52	2.007

[a] From reference [36].

We also investigated the possibility that the carbonyl group of the acetate substituent fills the sixth coordination position at Co^{III}, yielding a more stable octahedral complex, [$Co(acac)_2${(κ^2:*C*,*O*)-$CH(CH_3)(COOCH_3)$}], as the NMR spectroscopic study suggests that this may be the structure adopted by the chain end in the dormant state. Indeed, formation of the five-membered ring stabilizes the X= $OOCCH_3$ system by over six additional kcal mol^{-1}. The optimized geometry is also shown in Figure 15. Note that the $Co(acac)_2$ geometry has rearranged to make two mutually *cis* coordination sites available for the alkyl group chelation. An analogous stabilization is not possible for the X= COOMe system, because this would lead to a strained four-membered ring. Indeed, we find that the local minimum for such a [$Co(acac)_2${(κ^2:*C*,*O*)-$CH(CH_3)(COOCH_3)$}] model system has a higher energy than the (κ^1:C) minimum shown in Figure 15. To conclude, DFT calculations support the suggestion that the PVAc–$Co(acac)_2$ dormant chain in the VAc CMRP (occurring via degenerative transfer in the absence of added Lewis base) contains a six-coordinate Co^{III} center in which the growing PVAc chain adopts a chelating coordination mode, as represented in Figures 3a and 15.

Conclusion

We have reported for the first time the isolation of low-molecular-weight cobalt adducts formed at the very early stage of the CMRP of VAc. A combination of spectroscopic studies, DFT calculations, and polymerization tests allowed us to understand how the $Co(acac)_2$/V-70 pair initiates and controls this radical polymerization (Scheme 4).

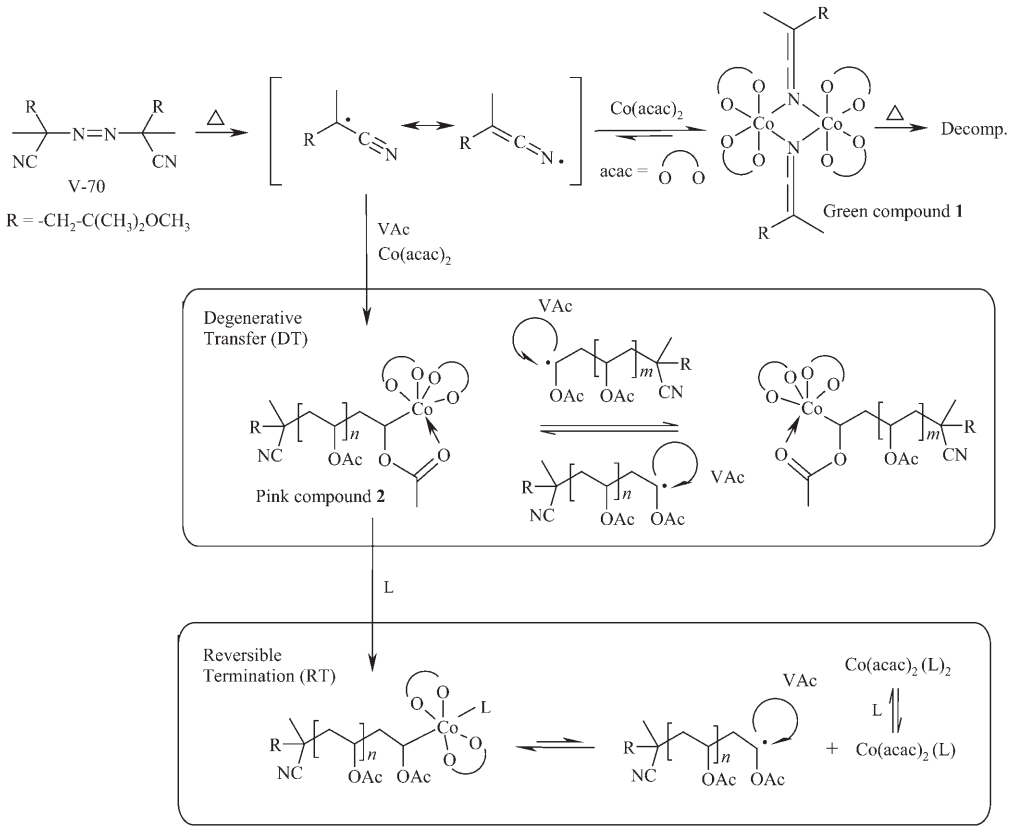

Scheme 4. Summary of the CMRP-initiating system.

Briefly, two cobalt adducts are formed in the polymerization medium during the induction period, namely, a minor green compound identified as a ketiminatocobalt dimer complex prone to decomposition and a major pink derivative that is an oligomer, end-capped by $Co(acac)_2$ containing an average of four VAc units (Scheme 4). According to DFT calculations, the carbonyl group of the terminal VAc unit of the pink derivative is coordinated to cobalt, which stabilizes the complex. In contrast to the green compound, the pink PVAc–$Co(acac)_2$ oligomer is a very efficient CMRP initiator and the VAc polymerization is then very slow. However, the addition of V-70 to the polymerization medium increases the polymerization rate while maintaining reasonable control, which supports the idea that the system is then dominated by a degenerative chain-transfer mechanism. Moreover, a dramatic increase in the polymerization rate can also be triggered by ligating Co with pyridine or water. Parallel to this favorable kinetic effect, the best control ever achieved of the polymerization of VAc is observed. In this case, the CMRP process proceeds through a reversible-termination mechanism. The role of the Lewis base is to saturate the free coordination site left available by Co^{III}–C bond rupture, as previously established.[36] The Co^{II} species is energetically stabilized and the radical formation equilibrium is shifted to the right.

Finally, it is clear now that water plays a key role whenever CMRP is carried out in aqueous dispersed media. The in-depth analysis of the CMRP mechanism reported in this work is the best lever possible for CMRP to contribute effectively to the macromolecular engineering of usually reluctant polymers.

Experimental Section

Materials: VAc (>99%, Acros) was dried over calcium hydride, degassed by several freeze–thaw cycles, distilled under reduced pressure, and stored under argon. Ethyl acetate (EtOAc) and dichloromethane (CH_2Cl_2) were dried over molecular sieves and degassed by bubbling argon for 30 min. V-70 (Wakko), $Co(acac)_2$ (>98%, Acros), TEMPO (98%, Aldrich), and pyridine (Aldrich, > 99%) were used as received.

Characterization: ^{1}H NMR spectra were recorded with a Bruker AM 250 spectrometer (250 MHz) in deuterated chloroform. IR spectra were recorded with a Perkin–Elmer FTIR instrument in the 4000 to 600 cm^{-1} range. Low-molecular-weight cobalt adducts were dissolved in CH_2Cl_2 and solvent-cast on a NaCl disk before IR spectroscopic analysis. Inductively coupled plasma mass spectrometry (ICP-MS) was carried out with an Elan DRC-e Perkin–Elmer SCIEX spectrometer. Samples were prepared as follows: the cobalt adduct stock solution (1 mL) in CH_2Cl_2 was allowed to evaporate, the residue was treated with HNO_3 (1 mL, 65%) at 60°C for 2 h, and the reaction mixture was diluted with twice-distilled water (250 mL). UV/vis spectra were recorded with a Hewlett–Packard 8453 spectrophotometer, by using the pure solvent as a reference. Size-exclusion chromatography (SEC) of PVAc was carried out in THF (flow rate: 1 mL min^{-1}) at 40°C with a Waters 600 liquid chromatograph equipped with a 410 refractive index detector and styragel HR columns (four columns HP PL gel 5 μm, 10^5, 10^4, 10^3, and 10^2 Å).

Synthesis and recovery of cobalt(III) adducts 1 and 2: $Co(acac)_2$ (10 g, 39 mmol) and V-70 (9.25 g, 31 mmol) were added to a round-bottomed flask capped by a three-way stopcock and purged by three vacuum–argon cycles. After the addition of degassed VAc (75 mL, 813 mmol), the reaction mixture was heated at 30 °C with stirring for 70 h. The medium remained pink throughout the polymerization, and no increase in viscosity was observed. The residual monomer was then evaporated under reduced pressure at room temperature, and the residue was placed under argon before being dissolved (or at least dispersed) in dry and degassed CH_2Cl_2. The solution was then transferred with a cannula to the top of a silica-gel column prepared as follows. A column, equipped with a three-way stopcock at the top and a 1 L flask at the bottom, was filled with silica, with the assistance of CH_2Cl_2 eluant. The column was placed under argon and eluted with dry, degassed CH_2Cl_2 (1 L) before the crude reaction product was deposited for chromatographic separation, while avoiding any exposure to air. After the elimination of V-70 residue with CH_2Cl_2, a green fraction was collected with CH_2Cl_2/EtOAc (85:15) as eluant. Finally, a pink fraction was eluted with EtOAc. The two fractions were evaporated to dryness, and the collected green cobalt adduct **1** and pink cobalt adduct **2** were stored at −20 °C under argon before stock solutions were prepared for analysis. Adducts **1** and **2** were dissolved, respectively, in 4 and 10 mL of degassed CH_2Cl_2. The cobalt concentration of these solutions was measured by ICP ($[Co(\mathbf{1})] = 1.40 \times 10^{-1}$ M and $[Co(\mathbf{2})] = 2.27 \times 10^{-1}$ M).

Synthesis of cobalt complex 1 in the absence of VAc: $Co(acac)_2$ (5.00 g, 20.0 mmol) and V-70 (4.60 g, 15.5 mmol) were added to a round-bottomed flask capped by a three-way stopcock and purged by three vacuum–argon cycles. After addition of degassed and distilled anisole (50.0 mL, 46.7 g, 542 mmol), the reaction mixture was heated at 30 °C under stirring for 120 h. The solvent was then evaporated under reduced pressure at 30 °C and the crude mixture was eluted through silica gel under an inert atmosphere as aforementioned. After elimination of V-70 by elution with degassed CH_2Cl_2, a green compound **1** was recovered with CH_2Cl_2/EtOAc (85:15) as eluant. No pink compound was collected by elution with EtOAc. This fraction was evaporated to dryness under reduced pressure and analyzed by IR, NMR, and UV spectroscopy.

Reaction of pink cobalt adduct 2 with TEMPO: Under an inert atmosphere, adduct **2** (0.33 mmol, estimated by ICP) and a tenfold molar excess of TEMPO (500 mg, 3.2 mmol) were dissolved in absolute ethanol (20 mL), previously degassed by bubbling of argon through for 20 min. The solution was then heated at 50 °C for 24 h. Upon cooling to room temperature, the released $Co(acac)_2$ crystallized and was eliminated by filtration. After solvent evaporation under reduced pressure at 72 °C, the reaction mixture was analyzed by ^1H NMR spectroscopy with $CDCl_3$.

VAc polymerization initiated by the cobalt(III) adducts: Pink cobalt adduct **2** solution (1 mL, $[Co] = 2.27 \times 10^{-1}$ M, 0.227 mmol) was added to a round-bottomed flask capped by a three-way stopcock, purged by three vacuum–argon cycles, and evaporated to dryness under reduced pressure. Again under an argon atmosphere, degassed VAc (5 mL, 4.67 g, 54.2 mmol) was added and the reaction mixture was heated at 30 °C under stirring. Samples were regularly collected and both the monomer conversion (gravimetry) and the molecular weight of PVAc (SEC) were determined. Prior to analyses, a tiny amount of TEMPO was added to each sample to prevent post-coupling reactions. The same experiment was repeated with the green compound **1** and the green low-molecular-weight adduct **3**, collected after exposure of the pink compound **2** to air (see the Results and Discussion).

VAc polymerization initiated by cobalt(III) adduct 2 in the presence of additives: Pink cobalt adduct **2** solution (1 mL, $[Co] = 2.27 \times 10^{-1}$ M, 0.227 mmol) was added to a round-bottomed flask capped by a three-way stopcock, purged by three vacuum–argon cycles, and evaporated to dryness under reduced pressure. Again under an argon atmosphere, degassed VAc (5 mL, 4.67 g, 54.2 mmol) was added, followed by V-70 (0.02 mmol), pyridine (0.229 mmol), or water (2.20 mmol), and the reaction mixture was heated at 30 °C whilst stirring. Samples were regularly collected from the polymerization medium to monitor both the monomer conversion (gravimetry) and the molecular weight of PVAc (SEC).

General recipe for the CMRP of VAc added with water at the end of the induction period: $Co(acac)_2$ (81 mg, 0.3 mmol) and V-70 (270 mg, 0.9 mmol) were added to a round-bottomed flask capped by a three-way stopcock and purged by three vacuum–argon cycles. After the addition of degassed VAc (15 mL, 14.04 g, 162 mmol), the reaction mixture was heated at 30 °C whilst stirring. After the induction period of 21 h, the monomer conversion was estimated at 4 % (gravimetry) and the pink polymerization medium was divided into three 4 mL parts (0.08 mmol of $Co(acac)_2$, 43.2 mmol of VAc). The first part was evaporated to dryness under vacuum at room temperature and then added with VAc (4 mL), previously saturated with water. The second portion was merely added with twice-distilled and degassed water (1 mL, $V_{VAc}/V_{H_2O} = 4$). Polymerization was kept running in the last fraction, which was therefore a reference. In all cases, polymerization was conducted at 30 °C under an inert atmosphere. Samples were regularly withdrawn and both the monomer conversion (gravimetry) and the molecular weight of PVAc (SEC) were determined.

Computational details: All geometry optimizations were performed by using the B3LYP three-parameter hybrid density functional method of Becke,[60] as implemented in the Gaussian 03 suite of programs.[61] The basis functions consisted of the standard 6-31G** for all light atoms (H, C, N, O) plus the LANL2DZ function, which included the Hay and Wadt effective core potentials,[62] for Co. The latter basis set was, however, augmented with an *f* polarization function ($\alpha = 0.8$) to obtain a balanced basis set and to improve the angular flexibility of the metal functions. All geometry optimizations were carried out without any symmetry constraint, and all final geometries were characterized as local minima of the potential energy surface by verifying that all second derivatives of the energy were positive. The unrestricted formulation was used for open-shell molecules. The mean value of the spin of the first-order electron wave function, which is not an exact eigenstate of S^2 for unrestricted calculations on open-shell systems, was considered to identify unambiguously the spin state. The value of $<S^2>$ at convergence was very close to the expected value of 0.75 for the radical species, indicating minor spin contamination. All energies were corrected for zero-point vibrational energy and for thermal energy to obtain the BDEs at 298 K. The standard approximations for estimating these corrections were used (ideal gas, rigid rotor, and harmonic oscillator) as implemented in Gaussian 03.

Acknowledgements

The authors from Liège are indebted to the "Belgian Science Policy" for financial support in the frame of the Interuniversity Attraction Poles Programme (PAI VI/27)—Functional Supramolecular Systems, and to the Fonds National de la Recherche Scientifique (F.N.R.S., Belgium). The authors thank Wako for kindly providing them with V-70. We are much indebted to M. Dejeneffe and G. Cartigny for skilful assistance. A.D. and C.D. are "Chargé de Recherche" and "Chercheur Qualifié" by the F.N.R.S., respectively. The authors from Toulouse wish to thank the "Agence National de la Recherche" (Contract No. NT05-2 42140) and the "Centre Interuniversitaire de Calcul de Toulouse" (Project CALMIP) for granting free computational time.

[1] W. A. Braunecker, K. Matyjaszewski, *Prog. Polym. Sci.* **2007**, *32*, 93–146.
[2] K. Matyjaszewski, J. Xia, *Chem. Rev.* **2001**, *101*, 2921–2990.
[3] M. Kamigaito, T. Ando, M. Sawamoto, *Chem. Rev.* **2001**, *101*, 3689–3745.
[4] G. Moad, J. Chiefari, Y. K. Chong, J. Krstina, R. T. A. Mayadunne, A. Postma, E. Rizzardo, S. H. Thang, *Polym. Int.* **2000**, *49*, 993–1001.
[5] G. Moad, E. Rizzardo, S. H. Thang, *Aust. J. Chem.* **2005**, *58*, 379–410.
[6] J. T. Lai, D. Filla, R. Shea, *Macromolecules* **2002**, *35*, 6754–6756.

[7] J. Chiefari, Y. K. Chong, F. Ercole, J. Krstina, J. Jeffery, T. P. T. Le, R. T. A. Mayadunne, G. F. Meijs, C. L. Moad, G. Moad, E. Rizzardo, S. H. Thang, *Macromolecules* **1998**, *31*, 5559–5562.
[8] S. Perrier, P. Takolpuckdee, C. A. Mars, *Macromolecules* **2005**, *38*, 2033–2036.
[9] M. K. Georges, R. P. N. Veregin, P. M. Kazmaier, G. K. Hamer, *Macromolecules* **1993**, *26*, 2987–2988.
[10] C. J. Hawker, A. W. Bosman, E. Harth, *Chem. Rev.* **2001**, *101*, 3661–3688.
[11] S. Grimaldi, J.-P. Finet, F. Le Moigne, A. Zeghdaoui, P. Tordo, D. Benoit, M. Fontanille, Y. Gnanou, *Macromolecules* **2000**, *33*, 1141–1147.
[12] D. Benoit, V. Chaplinski, R. Braslau, C. J. Hawker, *J. Am. Chem. Soc.* **1999**, *121*, 3904–3920.
[13] Y. Kwak, A. Goto, T. Fukuda, Y. Kobayashi, S. Yamago, *Macromolecules* **2006**, *39*, 4671–4679.
[14] S. Yamago, B. Ray, K. Iida, J. Yoshida, T. Tada, K. Yoshizawa, Y. Kwak, A. Goto, T. Fukuda, *J. Am. Chem. Soc.* **2004**, *126*, 13908–13909.
[15] S. Yamago, E. Kayahara, M. Kotani, B. Ray, Y. Kwak, A. Goto, T. Fukuda, *Angew. Chem.* **2007**, *119*, 1326–1328; *Angew. Chem. Int. Ed.* **2007**, *46*, 1304–1306.
[16] T. C. Chung, W. Janvikul, H. L. Lu, *J. Am. Chem. Soc.* **1996**, *118*, 705–706.
[17] T. C. Chung, H. Hong, Z. C. Zhang, Z. M. Wang, *ACS Symp. Ser.* **2006**, *944*, 387–403.
[18] J.-R. Caille, A. Debuigne, R. Jerome, *Macromolecules* **2005**, *38*, 27–32.
[19] R. Poli, *Angew. Chem.* **2006**, *118*, 5180–5192; *Angew. Chem. Int. Ed.* **2006**, *45*, 5058–5070.
[20] B. B. Wayland, G. Poszmik, S. L. Mukerjee, M. Fryd, *J. Am. Chem. Soc.* **1994**, *116*, 7943–7944.
[21] B. B. Wayland, L. Basickes, S. Mukerjee, M. Wei, M. Fryd, *Macromolecules* **1997**, *30*, 8109–8112.
[22] B. B. Wayland, S. Mukerjee, G. Poszmik, D. C. Woska, L. Basickes, A. A. Gridnev, M. Fryd, S. D. Ittel, *ACS Symp. Ser.* **1998**, *685*, 305–315.
[23] B. B. Wayland, X. Fu, Z. Lu, M. Fryd, *Polym. Prepr. Am. Chem. Soc. Div. Polym. Chem.* **2005**, *46*, 370–371.
[24] B. B. Wayland, C.-H. Peng, X. Fu, Z. Lu, M. Fryd, *Macromolecules* **2006**, *39*, 8219–8222.
[25] C.-H. Peng, M. Fryd, B. B. Wayland, *Macromolecules* **2007**, *40*, 6814–6819.
[26] A. Debuigne, J.-R. Caille, R. Jerome, *Angew. Chem.* **2005**, *117*, 1125–1128; *Angew. Chem. Int. Ed.* **2005**, *44*, 1101–1104.
[27] A. Debuigne, J.-R. Caille, C. Detrembleur, R. Jerome, *Angew. Chem.* **2005**, *117*, 3505–3508; *Angew. Chem. Int. Ed.* **2005**, *44*, 3439–3442.
[28] C. Detrembleur, A. Debuigne, R. Bryaskova, B. Charleux, R. Jerome, *Macromol. Rapid Commun.* **2006**, *27*, 37–41.
[29] A. Debuigne, J.-R. Caille, N. Willet, R. Jerome, *Macromolecules* **2005**, *38*, 9488–9496.
[30] R. Bryaskova, N. Willet, A. Debuigne, R. Jerome, C. Detrembleur, *J. Polym. Sci. Part A Polym. Chem.* **2006**, *45*, 81–89.
[31] R. Bryaskova, N. Willet, P. Degee, P. Dubois, R. Jerome, C. Detrembleur, *J. Polym. Sci. Part A Polym. Chem.* **2007**, *45*, 2532–2542.
[32] A. Debuigne, N. Willet, R. Jerome, C. Detrembleur, *Macromolecules* **2007**, *40*, 7111–7118.
[33] H. Kaneyoshi, K. Matyjaszewski, *Macromolecules* **2005**, *38*, 8163–8169.
[34] H. Kaneyoshi, K. Matyjaszewski, *Macromolecules* **2006**, *39*, 2757–2763.
[35] C. Detrembleur, O. Stoilova, R. Bryaskova, A. Debuigne, A. Mouithys-Mickalad, R. Jerome, *Macromol. Rapid Commun.* **2006**, *27*, 498–504.
[36] S. Maria, H. Kaneyoshi, K. Matyjaszewski, R. Poli, *Chem. Eur. J.* **2007**, *13*, 2480–2492.
[37] A. Debuigne, C. Detrembleur, R. Bryaskova, J.-R. Caille, R. Jerome, *ACS Symp. Ser.* **2006**, *944*, 372–386.
[38] R. H. Abeles, D. Dolphin, *Acc. Chem. Res.* **1976**, *9*, 114–120.
[39] K. P. Jensen, U. Ryde, *J. Am. Chem. Soc.* **2005**, *127*, 9117–9128.
[40] G. N. Schrauzer, R. J. Windgassen, *J. Am. Chem. Soc.* **1966**, *88*, 3738–3743.
[41] G. N. Schrauzer, *Angew. Chem.* **1976**, *88*, 465–474; *Angew. Chem. Int. Ed. Engl.* **1976**, *15*, 417–426.
[42] L. Randaccio, *Comments Inorg. Chem.* **1999**, *21*, 327–376.
[43] K. H. Reddy, *Resonance* **1999**, *4*, 67–77.
[44] R. D. W. Kemmitt, D. R. Russell in *Comprehensive Organometallic Chemistry, Vol. 5* (Eds.: G. Wilkinson, F. G. A. Stone, E. W. Abel), Pergamon, Oxford, **1982**, pp. 1–276.
[45] J. E. Huheey, E. A. Keiter, R. L. Keiter in *Inorganic Chemistry: Principles of Structure and Reactivity*, 4th ed., Harper & Row, New York, **1993**.
[46] E. Pretsch, T. Clerc, J. Seibl, W. Simon, *Spectral Data for Structure Determination of Organic Compounds*, 2nd ed., Springer, Berlin, **1983**.
[47] D. M. Tellers, J. C. M. Ritter, R. G. Bergman, *Inorg. Chem.* **1999**, *38*, 4810–4818.
[48] J. R. Fulton, M. W. Bouwkamp, R. G. Bergman, *J. Am. Chem. Soc.* **2000**, *122*, 8799–8800.
[49] J. R. Fulton, S. Sklenak, M. W. Bouwkamp, R. G. Bergman, *J. Am. Chem. Soc.* **2002**, *124*, 4722–4737.
[50] G. J. Kruger, E. C. Reynhardt, *Acta Crystallogr. Sect. B: Struct. Crystallogr. Cryst. Chem.* **1974**, *30*, 822–824.
[51] K. G. Caulton, *New J. Chem.* **1994**, *18*, 25–41.
[52] A. R. Rossi, R. Hoffmann, *Inorg. Chem.* **1975**, *14*, 365–374.
[53] A. Debuigne, J.-R. Caille, R. Jerome, *Macromolecules* **2005**, *38*, 5452–5458.
[54] W. Mikolaiski, G. Baum, W. Massa, R. W. Hoffmann, *J. Organomet. Chem.* **1989**, *376*, 397–405.
[55] H. Fischer, *Macromolecules* **1997**, *30*, 5666–5672.
[56] T. Fukuda, A. Goto, K. Ohno, *Macromol. Rapid Commun.* **2000**, *21*, 151–165.
[57] A. Goto, T. Fukuda, *Prog. Polym. Sci.* **2004**, *29*, 329–385.
[58] M. B. Gillies, K. Matyjaszewski, P.-O. Norrby, T. Pintauer, R. Poli, P. Richard, *Macromolecules* **2003**, *36*, 8551–8559.
[59] K. Matyjaszewski, R. Poli, *Macromolecules* **2005**, *38*, 8093–8100.
[60] A. D. Becke, *J. Chem. Phys.* **1993**, *98*, 5648–5652.
[61] Gaussian 03 (Revision C.02), M. J. Frisch, G. W. Trucks, H. B. Schlegel, G. E. Scuseria, M. A. Robb, J. R. Cheeseman, J. A. Montgomery, Jr., T. Vreven, K. N. Kudin, J. C. Burant, J. M. Millam, S. S. Iyengar, J. Tomasi, V. Barone, B. Mennucci, M. Cossi, G. Scalmani, N. Rega, G. A. Petersson, H. Nakatsuji, M. Hada, M. Ehara, K. Toyota, R. Fukuda, J. Hasegawa, M. Ishida, T. Nakajima, Y. Honda, O. Kitao, H. Nakai, M. Klene, X. Li, J. E. Knox, H. P. Hratchian, J. B. Cross, C. Adamo, J. Jaramillo, R. Gomperts, R. E. Stratmann, O. Yazyev, A. J. Austin, R. Cammi, C. Pomelli, J. W. Ochterski, P. Y. Ayala, K. Morokuma, G. A. Voth, P. Salvador, J. J. Dannenberg, V. G. Zakrzewski, S. Dapprich, A. D. Daniels, M. C. Strain, O. Farkas, D. K. Malick, A. D. Rabuck, K. Raghavachari, J. B. Foresman, J. V. Ortiz, Q. Cui, A. G. Baboul, S. Clifford, J. Cioslowski, B. B. Stefanov, G. Liu, A. Liashenko, P. Piskorz, I. Komaromi, R. L. Martin, D. J. Fox, T. Keith, M. A. Al-Laham, C. Y. Peng, A. Nanayakkara, M. Challacombe, P. M. W. Gill, B. Johnson, W. Chen, M. W. Wong, C. Gonzalez, J. A. Pople, Gaussian, Inc., Wallingford, CT, **2004**.
[62] P. J. Hay, W. R. Wadt, *J. Chem. Phys.* **1985**, *82*, 270–283.

Received: November 27, 2007
Published online: March 3, 2008

